ELSEVIER

Materials Science and Engineering B86 (2001) 70–78

MATERIALS SCIENCE & ENGINEERING B

www.elsevier.com/locate/mseb

Impedance study of $SrBi_2Ta_2O_9$ and $SrBi_2(Ta_{0.9}V_{0.1})_2O_9$ ferroelectrics

Yun Wu, Mike J. Forbess, Seana Seraji, Steven J. Limmer, Tammy P. Chou, Guozhong Cao *

University of Washington, Materials Science and Engineering, Seattle, WA 98195, USA

Accepted 27 April 2001

Abstract

This paper reports the electrical impedance properties of strontium bismuth tantalates (SBT) and strontium bismuth tantalate vanadate (SBTV) ferroelectric ceramics. AC impedance analysis was used to study the influences of vanadium doping and post sintering annealing on the microstructure and electrical properties. It was found that the vanadium doping resulted in the formation of fine-grained microstructure and an appreciable increase in dielectric constants, and Curie temperature. Post sintering annealing led to an increase in dielectric constants, but a reduction in dc conductivity. Possible mechanisms of the influences of vanadium doping and post sintering annealing on the electrical properties are discussed.

Keywords: Impedance; Annealing; Ferroelectrics; Dielectrics

1. Introduction

Bismuth layer structured ferroelectrics (BLSF) have attracted a lot of research interest recently. Among the BLSFs, strontium bismuth tantalate (SBT) and strontium bismuth niobate (SBN) are the most promising fatigue free candidate materials for nonvolatile ferroelectric memory devices [1–3]. The dielectric and electric properties of the SBT system were widely studied in bulk materials and thin films [4–6]. In order to understand the electrical conduction mechanisms that control the polycrystalline SBT ceramics, the contributions from bulk and grain boundaries have to be separated. Frequency-dependent impedance measurements could deconvolute the two contributions and have been widely used in the study of electronic ceramics [7–9]. Desu et al. proposed an oxygen vacancy related low resistivity model to explain the fatigue free properties of SBT and SBN ferroelectrics, based on impedance study [10]. We have demonstrated that the partial substitution of tantalum and niobium ions by pentavalent vanadium ions has a profound influence on the dielectric and ferroelectric properties of SBN and SBT ferroelectrics [11,12]. It was also found that the partial substitution of niobium ions by vanadium ions has an appreciable influence on the electrical conductivity [13]. Furthermore, post-sintering annealing was found to have a significant influence on the dielectric properties of vanadium doped SBN ferroelectrics [14].

The present article is to report the electrical impedance study on the influences of vanadium doping and post-sintering annealing on the electrical and dielectric properties of SBT ceramics. In addition, attention was paid to the effects of vanadium doping and post-sintering annealing on the crystallinity and microstructure of SBT ceramics. The influences of postsintering annealing and vanadium doping on the properties of grains and grain boundary of SBT ceramics have been elaborated.

2. Experimental

Polycrystalline strontium bismuth tantalate, $SrBi_2Ta_2O_9$ (SBT), and strontium bismuth vanadium

* Corresponding author.
E-mail address: gzcao@u.washington.edu (G. Cao).

0921-5107/01/$ - see front matter
PII: S0921-5107(01)00657-2

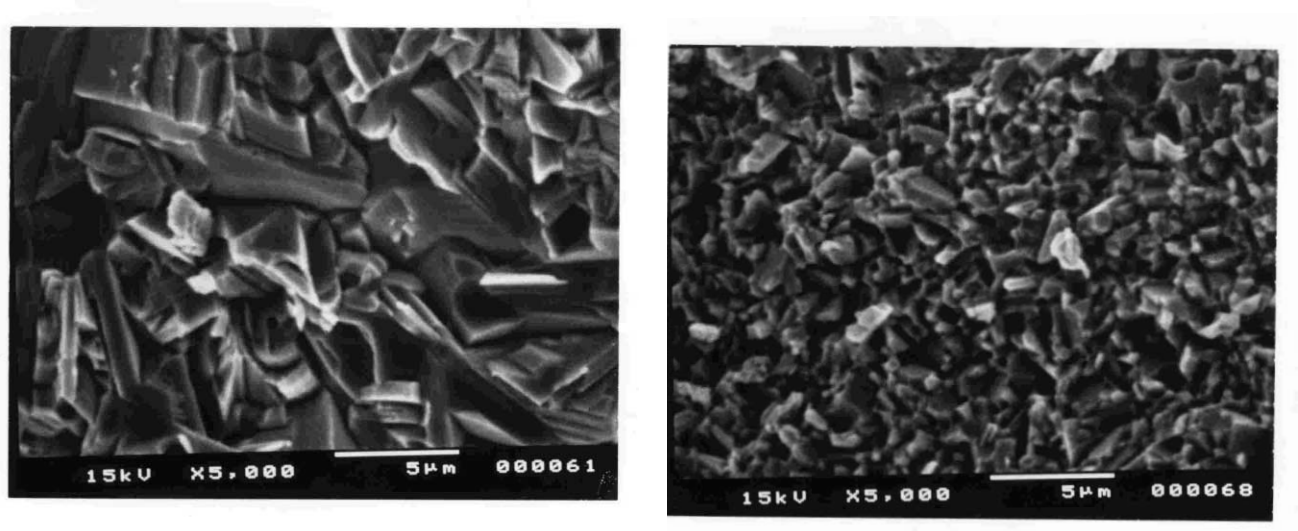

Fig. 1. SEM pictures of as sintered SBT (left) and SBTV (right) ceramics.

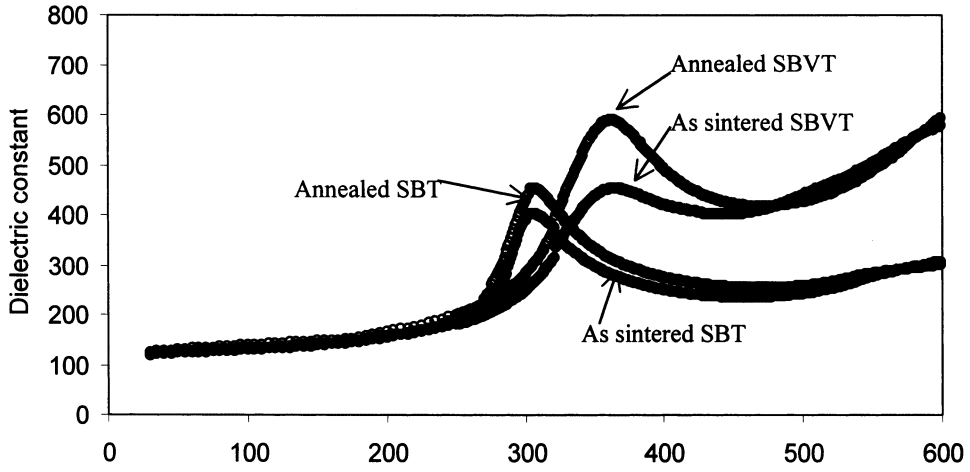

Fig. 2. Dielectric constants versus temperature for as sintered and post annealed SBT and SBTV ceramics at 100 kHz.

tantalate, $SrBi_2(Tao_{0.9}V_{0.1})_2O_9$ (SBTV), samples were prepared by solid state reaction sintering. The starting materials used were $SrCO_3$, Bi_2O_3, V_2O_5, and Ta_2O_5 (Aldrich Chem. Co.), all with a purity of 99%. The powders were admixed with a desired weight ratio with approximately 3.5 wt.% excess Bi_2O_3, which was to compensate weight loss of Bi_2O_3 due to its high vapor pressure (750 mm Hg at 1570 °C) [15]. Powders were ball-milled, dried, and then fired in air for 2 h at 850°C for SBTV and 1000 °C for SBT powders in covered crucibles. The fired powders were ground, admixed with approximately 1–1.5 wt.% Polyvinylalcohol (PVA, Aldrich Chem. Co.) as binder, and pressed into pellets by cold-isotropic pressing at 250 MPa. The pellets were sintered in closed crucibles for 2 h at 1000 °C for SBTV samples and 1200 °C for SBT samples in air. A relative density above 95% was achieved for both SBT and SBTV samples. The total weight loss was found to be around 7 wt.%, including the loss of CO_2 as a result of calcination of $SrCO_3$, the pyrolysis of PVA binder, and the evaporation of relatively volatile Bi_2O_3. The loss of Bi_2O_3 is estimated to be 2.7 wt.%, below the 3.5 wt.% excess Bi_2O_3 initially added into the system. Post sintering annealing was performed for 60 h in air at 1050 °C for SBT samples and 850 °C for SBTV samples. No appreciable change in relative density was found in both SBT and SBTV samples after annealing. Further, there was no weight-loss found after the annealing.

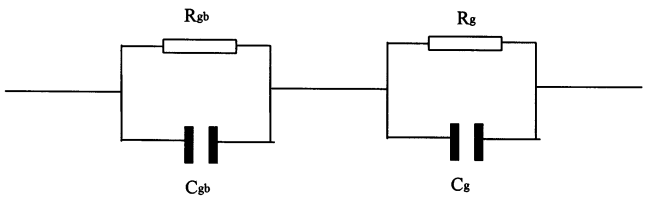

Fig. 3. Equivalent circuit of the studied ceramic system.

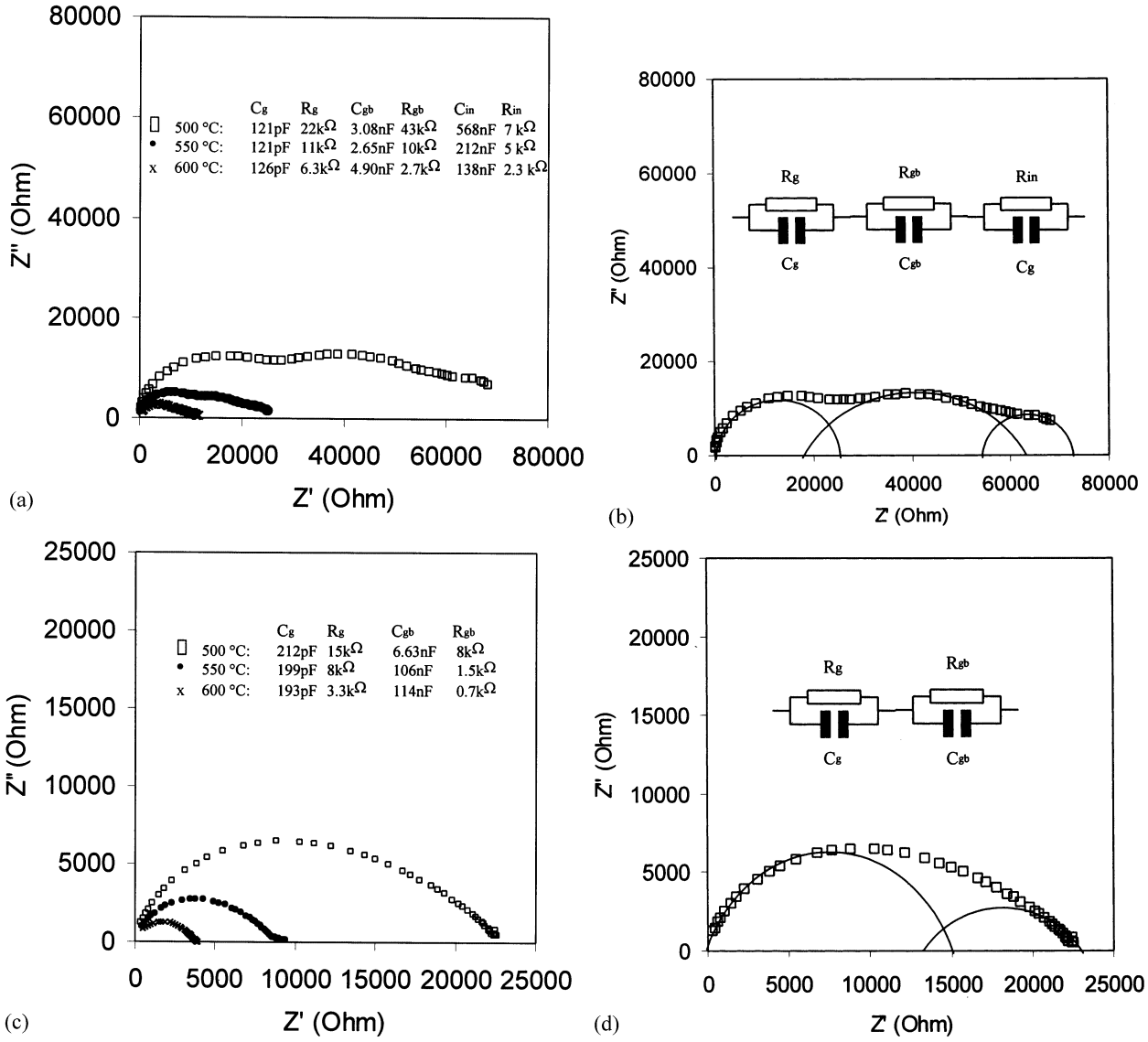

Fig. 4. Complex impedance plane plots at different temperatures for as sintered (a,b) SBT and SBTV (c,d).

X-ray diffraction data were obtained using CuKα radiation. SEM (JSM-5200) was used to analyze the micro structure of the ceramics. The pellets (10 mm in diameter) were polished to a thickness of approximately 1 mm and electroded by silver paste on both sides and cured at about 550 °C for about 30 min on a hot plate. The impedance measurements were carried out in the temperature range 250–600 °C using a Hewlett–Packard 4284A Precision LCR meter with 50 mV signal voltage and frequencies ranging from 20 to 10^6 Hz.

3. Results and discussion

X-ray diffraction analyses indicated both SBT and SBTV ceramics consisted of a single crystalline layered perovskite phase without any detectable secondary phase. Further, there was no appreciable difference in the lattice constants between the SBT and SBTV samples, though the radius of V^{5+} (58 pm) is significantly smaller than that of Ta^{5+} (69 pm) [16]. Similar results were found in the SBN system when the concentration of vanadium was less than 10%, which was attributed to the structural constraint imposed by the $Bi_2O_2^{2+}$ layers [17]. Post-sintering annealing was found having no appreciable influence on the XRD spectra of both SBT and SBTV samples, indicating that the annealing resulted in no detectable change in crystallinity or microstructure in both SBT and SBTV systems.

Fig. 1 is the SEM images of the fracture surfaces of SBT and SBTV ceramics without annealing. The fracture surfaces of both samples show dense structures, which is in a good agreement with above 95% theoretical density that was determined by Archimedes method. Further, both SBT and SBTV samples have shown a typical intergranular fracture, i.e. fracture propagates

along grain boundaries. However, the grain sizes in the SBT and SBTV samples differ significantly. The average grain size of the SBT ceramics is approximately 2 μm and twice the grain size of the SBTV samples (~ 1 μm). Although, it is not known what is the exact explanation for such markedly different grain size, the different sintering temperature and the partial substitution of tantalum ions by vanadium ions are possible causes. The sintering temperature of 1200 °C, for the SBT samples was 200 °C higher than that of the SBTV

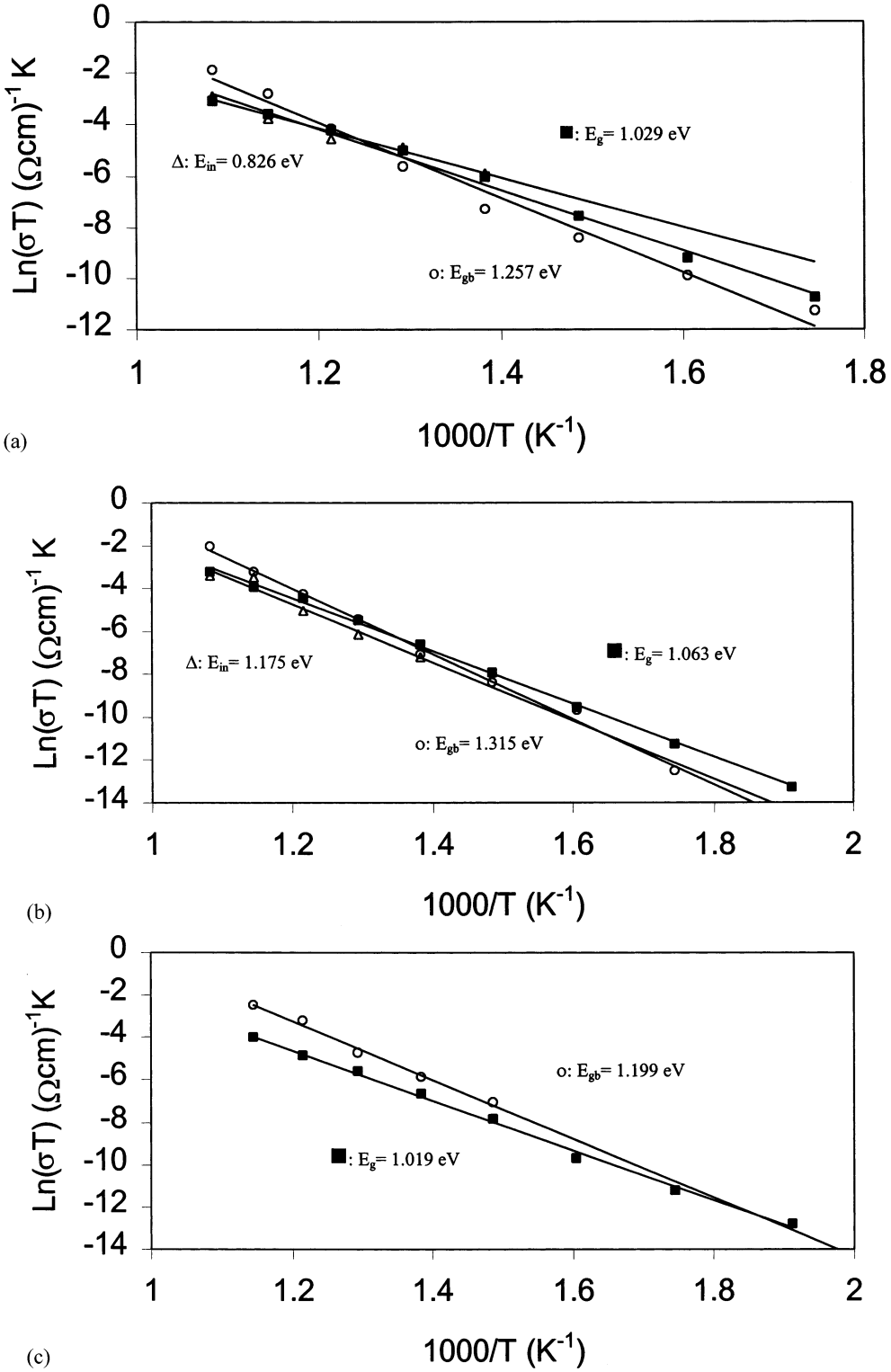

Fig. 5. Variation of conductivity from grain (□) and grain boundary (○) with temperature for as sitnered and annealed SBT (a,b); SBT (c,d) respectively.

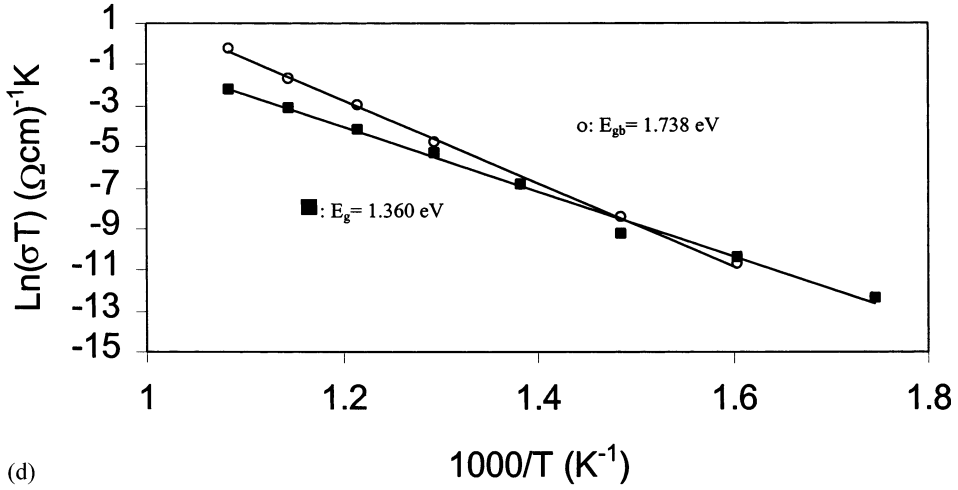

Fig. 5. (*Continued*)

Table 1
Compositions, sintering condition, and the activation energies of the SBT and SBTV ceramics

Sample	Processing condition	σ (grain) 500°C(Ω cm^{-1})	σ (grain boundary) 500°C(Ω cm^{-1})	*E*a (grain) (eV)	*E*a (grain boundary) (eV)	*E*a (interface) (eV)
SBT-as sintered	1200 °C-2 h	8.904×10^{-6}	4.556×10^{-6}	1.029	1.257	0.826
SBT-annealed	1050 °C-60 h	5.40×10^{-6}	5.581×10^{-6}	1.063	1.315	1.175
SBTV-as sintered	1000 °C-2 h	4.975×10^{-6}	1.137×10^{-5}	1.019	1.199	
SBTV-annealed	850 °C-60h	6.61×10^{-6}	1.1×10^{-5}	1.360	1.738	

samples (1000°C). It is well known that the grain growth becomes predominant at higher temperatures due to the fact that the activation energy of cross grain boundary diffusion is higher than that of the activation energy of grain-boundary diffusion for densification [18]. Therefore, a higher sintering temperature would result in a larger average grain size. The incorporation of vanadium into the system may also have a significant influence on the grain size. The incorporation of vanadium may promote the formation of a low melting-point mixture at grain boundaries during sintering, which would effectively increase the diffusion distance between the grains, which would result in a small grain size in the sintered ceramics [19]. Reduced grain size by partial substitution was also commonly found in other ferroelectric materials [20]. It is very likely that both a lower sintering temperature and the addition of vanadium oxide contributed to the finegrained microstructure of the SBTV samples as compared with the SBT samples. It is not known which played a predominant role in suppressing the grain growth in the SBTV samples. However, SEM observation revealed that the post sintering annealing resulted in no appreciable change in the microstructures of both SBT and SBTV samples.

Fig. 2 shows the dielectric constants as a function of temperature of both SBT and SBTV ceramics without annealing and after annealing measured at a frequency of 100 kHz. For as sintered samples, although the R.T. dielectric constant of SBTV is the same as that of SBT ceramics, both Curie temperatures and peak dielectric constants differ significantly. Curie temperature changed from 305 °C for SBT to 364 °C for SBTV, whereas the peak dielectric constant changed from 400 for SBT to 450 for SBTV. Such changes might be attributed to the partial substitution of tantalum ions by smaller pentavalent vanadium ions [14]. These changes may also, at least partly, be attributed to the difference in microstructure and stress that is related to the grain size [20]. Although a similar trend was observed for annealed SBT and SBTV samples, annealing resulted in an appreciable increase in the peak dielectric constants with $\sim$440 as compared with $\sim$400 for SBT and $\sim$610 as compared with $\sim$450 for the SBTV samples without annealing. However, it was found that Curie temperature of both SBT and SBTV samples remained almost unchanged after annealing.

No definite explanation was found for the change of the dielectric constants of both SBT and SBTV ceramics with annealing, however, several possible causes are

briefly discussed below. Post-sintering annealing would result in a reduction in residual stress in the samples, and thus lead to an increase in dielectric constants as reported in other ferroelectric systems [21]. Improved crystallinity and change of microstructure are also possible explanations, however, both XRD and SEM revealed no noticeable change in either crystallinity or microstructures. Change of chemical composition could be another possible cause. Although no weight loss was found, the color of the samples did change from dark brown to yellow brown after annealing, indicating there were possible changes in chemical composition or in valence states of constituent ions. For the SBTV samples, it is possible that the post-sintering annealing

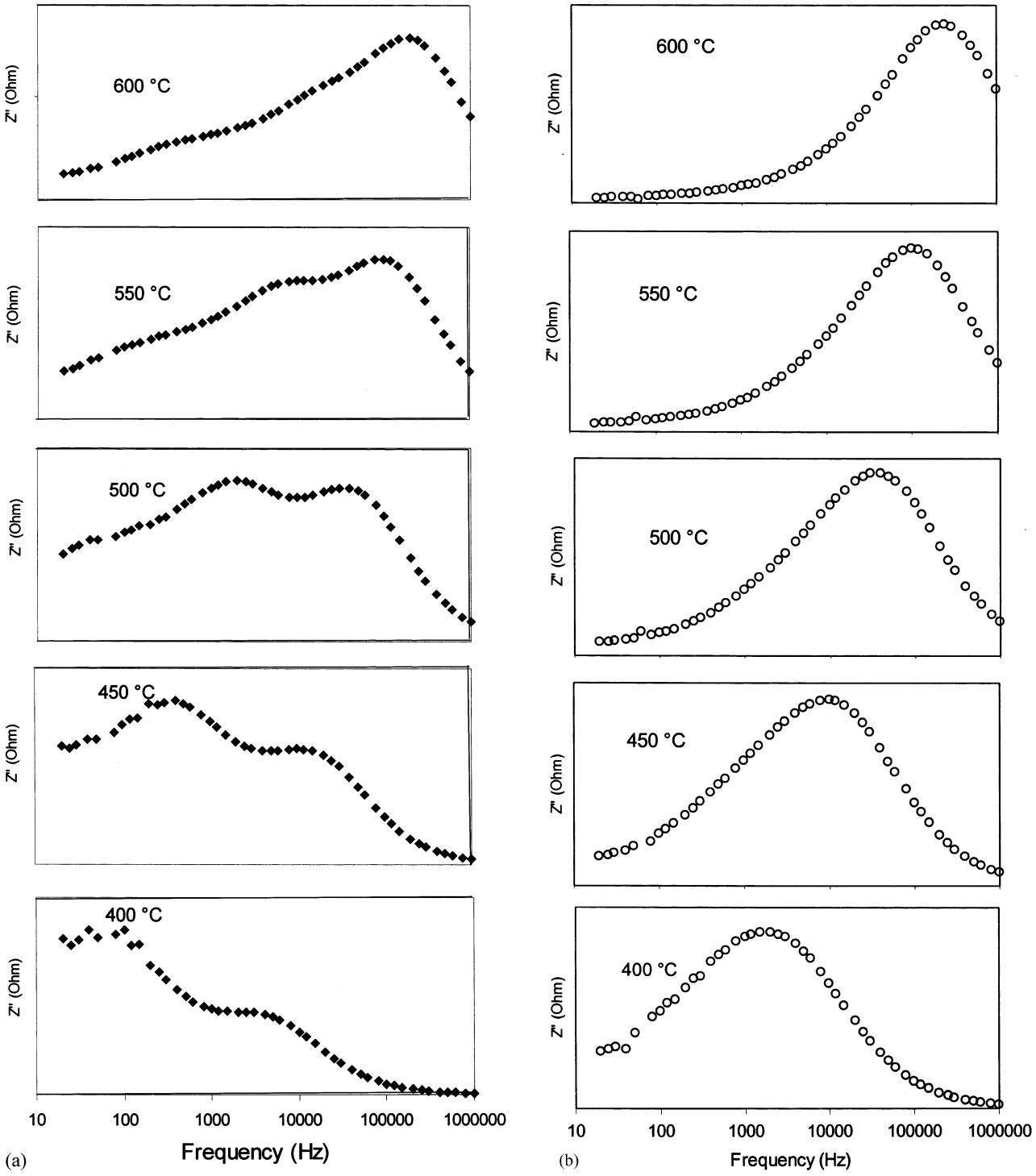

Fig. 6. Variation of reactance Z'' with frequency at different temperatures for as sintered SBT (a) and SBTV (b).

resulted in further oxidation of some tetravalent vanadium ions and thus reduction of oxygen vacancies in the system. However, the oxidation of tetravalent to pentavalent vanadium ions and the reduction of oxygen vacancies would result in an increase in both the peak dielectric constant and Curie point as discussed in detail elsewhere [11]. In the current research, Curie temperature of SBTV was found unchanged after annealing. The lack of observable change in Curie temperature could be partly due to temperature measurements, which commonly include a few degrees of variation. Further, the annealing was conducted in air and, thus, an extensive oxidation reaction was not very likely and the reduction of oxygen vacancies could not be the predominant effect. Further prolonged annealing of SBTV samples for 160 h indeed revealed an increase in Curie temperature (~ 5 °C), implying that there was a possible oxidation of tetravalent vanadium ions.

To better understand the influences of vanadium incorporation and post-sintering annealing on the electrical and dielectric properties of the SBT and SBTV ceramics, ac impedance analyses were conducted to separate the possible contributions of grains and grain boundaries. A schematic model of polycrystalline SBT and SBVT ceramics was described by the equivalent circuit (as shown in Fig. 3), which was proposed in the literature [22,23]. The circuit consists of a series connection of two sub-circuits, one represents grains and another represents the grain boundary phase. Each sub-circuit is composed of one resistor and one capacitor in parallel. The impedance of such an equivalent circuit can be described by both the real part, Z', and the imaginary part, Z'' as follows [23]:

$$Z = \frac{R_g}{1+(\omega R_g C_g)^2} + \frac{R_g}{1+(\omega R_{gb} C_{gb})^2} \quad (1)$$

$$Z'' = R_g\left(\frac{\omega R_g C_g}{1+(\omega R_g C_g)^2}\right) + R_{gb}\left(\frac{\omega R_{gb} C_{gb}}{1+(\omega R_{gb} C_{gb})^2}\right) \quad (2)$$

where $\omega = 2\pi f$ is the angular frequency and C_g, R_g, C_{gb}, R_{gb} are the capacitance and resistance of grains and grain boundaries, respectively.

Fig. 4 shows the typical Z''–Z' plots of the SBT and SBTV samples without annealing at various temperatures. There are mainly two overlapping semicircles, which correspond to grains (the semicircle on the left-hand side) and grain boundaries (the semicircle on the right-hand side) in the SBT samples below 450 °C. When temperature is above 450 °C, there exist three overlapping semicircles (Fig. 4a). The lowest frequency range arc was attributed to be the ferro electric-electrode interface effect, which is similar with T. Chen et al.'s results [10]. When the temperature increases, all three semicircles become smaller and shift towards lower Z' values, indicating a reduction of grain, grain boundary and interface resistance [22]. Z''–Z' plot at 500 °C with fitting curves were shown in Fig. 4b. The typical Z''–Z' plots of the SBTV ferroelectrics shown in Fig. 4c were found to be rather different from those of the SBT samples shown in Fig. 4a. The Z''–Z' plots of the SBTV samples were predominated by a single semicircle with a little deviation at the low frequency range. The predominant semicircles represent the impedance contribution of the grains, whereas the grain boundaries have a less significant contribution to the impedance. As the temperature increases, the intercepts of the predominant semicircles at the Z' axis shift towards lower Z' values, indicating the reduction of the grain resistance. In addition, the deviations at low frequencies that correspond to the contribution of the grain boundaries decrease with an increasing temperature. Further, the depressed semicircles have their centers on a line far below the real axis, indicating departure from the ideal Debye behavior [24]. Another Z''–Z' plot for SBTV at 500 °C with fitting curves were shown in Fig. 4d.

Fig. 5 shows the Arrehenius plots of the conductivity of the SBT and SBTV sintered and annealed samples from different contributions as a function of temperature. The activation energies of both SBT and SBTV samples with and without annealing are summarized in Table 1. Also the conductivities of grain and grain boundary phases calculated from impedance at 500 °C are included in this Table for comparison. These data do not show much difference but our dc conductivity measurement did show decreasing conductivity results after annealing [12]. Fig. 5a and Fig. 5b are the conductivity results of the SBT ceramics with and without annealing. The conductivity results of the SBTV samples with and without annealing were shown in Fig. 5c and Fig. 5d. The influences of the incorporation of vanadium into the system are 2-fold: the reduction of the grain size as clearly demonstrated by the SEM images in Fig. 1, and the possibly enhanced concentration of oxygen vacancies. It is known that vanadium can have both pentavalent and tetravalent states. If there are some tetravalent vanadium ions that occupy the tantalum ions' positions, oxygen vacancies need to be created to maintain electroneutrality. Even in SBT ceramics, the evaporation of bismuth oxide during sintering would also produce oxygen vacancies. The activation energies of the conduction for SBT-as sintered, SBT-annealed and SBTV-as sintered range from 1.019–1.315 eV, which are reasonably in agreement with the data reported in the literature [25–27]. This indicates that the conduction could be attributed to the motion of the oxygen vacancies. However, the activation energies of conduction for annealed SBTV, especially for grain boundary part (1.738 eV) is difficult to be explained by the same mechanism. Actually further study is required for better understanding of the phenomenon.

Another noticeable change in both SBT and SBTV samples resulting from the annealing is the increase in the activation energy for both grain and grain boundary conduction. It is not known what is the exact mechanism for such a change. Although the incorporation of vanadium into the SBT crystal structure is expected to increase the complexity and thus to increase the activation energy of conduction, it could not explain the significant change of the activation energy with annealing, particularly the activation energy of grain boundary conduction. Annealing is likely to reduce the stress and strain in both grains and grain boundaries, however, it is not very likely that a reduction in stress would result in such a significant increase in activation energy for electrical conduction. Change in chemical composition, crystallinity, and microstructure would also result in a change of activation energy of diffusion, however, both XRD and SEM results revealed that there was no detectable change in crystallinity and microstructure of the SBTV ceramics with the annealing, as discussed earlier. Furthermore, no detectable weight loss implied that there was no or negligible change in chemical composition.

Fig. 6 shows the imaginary part of the impedance, Z'', as a function of frequency in both SBT and SBTV ceramics without annealing. Such plots would allow an in-depth study of the contribution of both grain and grain boundary phase on the conductivity and dielectric properties separately. Compared with bulk and grain boundary, the interface effect is much weaker, therefore, not shown in the spectroscopic plots. At 400 °C, SBT samples show two distinct peaks that correspond to contributions of the grain (at the high frequency side) and the grain boundary (on the low frequency side) phases, respectively. When the temperature increases, both peaks shift to higher frequencies. The grain boundary peak shifts faster than that of the grains; eventually two peaks merge together at 600 °C. The SBTV samples demonstrate a different relationship as shown in Fig. 6b. Similarly, the weaker contributions from the grain boundary were not shown in the plots. There is only one peak at temperatures ranging from 400 to 600 °C. This peak corresponding to the grain phase also shifts to higher frequencies as the temperature increases. Since the change of dielectric constant of the grain boundary phase would be relatively small, the shift of the peak towards higher frequencies, as the temperature increases, is mainly due to the reduction of bulk resistivity. Further analysis will be conducted to get a better understand of the influences of the incorporation of vanadium and the post-sintering annealing on the dielectric properties of the grain boundaries. Such experiments will be combined with detailed systematic analysis on the microstructures and chemical compositions of the grain boundary phase.

4. Conclusions

Partial substitution of tantalum ions by vanadium ions (10%) in the SBT system resulted in the formation of fine-grained microstructure and an increase in dielectric constants and DC conductivity. Post-sintering annealing had no appreciable influences on the chemical composition, crystallinity and micro structure of both SBT and SBTV ceramics. However, post-sintering annealing led to an appreciable increase in dielectric constants in both SBT and SBTV ceramics, most likely. due to reduced stress and oxidation of possible tetravalent vanadium ions.

Acknowledgements

The authors would like to thank PNNL (S. Limmer), Ford Motor Co. (S. Seraji), the Center for Nanotechnology at the University of Washington (Y. Wu and S. Seraji) for financial support.

References

[1] C.A.P. de Araujo, J.D. Cuchlaro, L.D. McMillan, M.C. Scott, J.F. Scott, Nature 374 (1995) 627.
[2] S.B. Desu, D.P. Vijay, Mater. Sci. Eng. B 32 (1995) 75.
[3] R.E. Jones Jr, P.D. Maniar, R. Moazzami, P. Zurcher, J.Z. Witowski, Y.T. Lii, P. Chu, S.J. Gillespie, Thin Solid Films 270 (1995) 584.
[4] Y. Torii, K. Tato, A. Tsuzuki, H.J. Hwang, S.K. Dey, J. Mater. Sci. Lett. 17 (1998) 827.
[5] N. Seong, C. Yang, W. Shin, S. Yoon, Appl. Phys. Lett. 72 (1998) 1374.
[6] R. Dat, J.K. Lee, O. Auciello, A.I. Kingon, Appl. Phys. Lett. 67 (1995) 572.
[7] R.D. Armstrong, T. Dickinson, P.M. Willis, J. Electroanal. Chem. 53 (1994) 389.
[8] D. Arcos, M. Vazquez, R. Valenzuela, M. Vallet-Regi, J. Mater. Res. 14 (1999) 861.
[9] T. Stratton, A. McHale, D. Button, H.L. Tuller, Materials science research, in: J. Pask, A. Evans (Eds.), Surfaces and Interfaces in Ceramic and Ceramic Metal System, vol. 14, Plenum, NewYork, 1981, pp. 77–81.
[10] T.C. Chen, C. Thio, S.B. Desu, J. Mater. Res. 12 (1997) 2628.
[11] Y. Wu, G.Z. Cao, Appl. Phys. Lett. 75 (1999) 2650.
[12] Y. Wu, M. Forbess, S. Seraji, S. Limmer, T. Chou, and G.Z. Cao, J. Phys. D. 89 (2001) 5647.
[13] Y. Wu, G.Z. Cao, J. Mater. Res. 15 (2000) 1583.
[14] Y. Wu, M. Forbess, S. Seraji, T. Chou, G.Z. Cao, J. Appl. Phys. (in press).
[15] R.C. Weast, M.J. Astle (Eds.), CRC Handbook of Chemistry and Physics, 61st Ed., CRC Press, Inc, Boca Raton, FL, 1974.
[16] R.D. Shannon, C.T. Prewitt, Acta Crystallogr. B 25 (1969) 925.
[17] Y. Wu, C. Nguyen, S. Seraji, M.J. Forbess, S.J. Limmer, T. Chou, G.Z. Cao, J. Am. Ceram. Soc. (in press).
[18] W.D. Kingery, H.K. Bower, D.R. Uhlmann, Introduction to

Ceramics, second Edn, Wiley, New York, 1976.
[19] R.G. German, Liquid Phase Sintering, Plenum Press, New York, 1985.
[20] A.J. Moulson, J.M. Herbert, Electroceramics, Chapman & Hall, London, 1990.
[21] F. Xia, X. Yao, J. Inorg. Mater. 14 (1999) 180.
[22] J.R. Macdonald, Impedance Spectroscopy, Wiley, NewYork, 1987 Chapter 4.
[23] D.C. Sinclair, A.R. West, J. Appl. Phys. 66 (1989) 3850.
[24] D.C. Sinclair, A.R. West, J. Mater. Sci. 29 (1994) 6061.
[25] A. Chen, Y. Zhi, L.E. Cross, Phys. Rev. B 62 (2000) 228.
[26] Y. Zhi, A. Chen, P.M. Vilarinho, P. Mantas, J.L. Baptista, J. Appl. Phys. 83 (1998) 4874.
[27] R. Waser, J. Am. Ceram. Soc. 74 (1991) 1934.